

1 **A total energy error analysis of dynamical cores and**
2 **physics-dynamics coupling in the Community Atmosphere**
3 **Model (CAM)**

4 **Peter H. Lauritzen^{1*}, and David L. Williamson¹**

5 ¹National Center for Atmospheric Research, Boulder, Colorado, USA

6 **Key Points:**

- 7 • Spurious total energy dissipation in dynamical core is $-0.3W/m^2$ to $-1W/m^2$ at 1
8 degree
9 • Constant-pressure assumption in physics leads to $0.3W/m^2$ spurious total energy
10 source
11 • There can easily be compensating errors in total energy budget

*1850 Table Mesa Drive, Boulder, Colorado, USA

Corresponding author: Peter Hjort Lauritzen, pel@ucar.edu

12 **Abstract**

13 A closed total energy (TE) budget is of utmost importance in coupled climate system
 14 modeling; in particular, the dynamical core or physics-dynamics coupling should ideally
 15 not lead to spurious TE sources/sinks. To assess this in a global climate model, a detailed
 16 analysis of the spurious sources/sinks of TE in NCAR's Community Atmosphere Model
 17 (CAM) is given. This includes spurious sources/sinks associated with the parameteriza-
 18 tion suite, the dynamical core, TE definition discrepancies and physics-dynamics coupling.
 19 The latter leads to a detailed discussion of the pros and cons of various physics-dynamics
 20 coupling methods commonly used in climate/weather modeling.

21 **1 Introduction**

22 In coupled climate modeling with prognostic atmosphere, ocean, land, land-ice, and
 23 sea-ice components, it is important to conserve total energy (TE) to a high degree in each
 24 component individually and in the complete model to avoid spurious long term trends in
 25 the simulated Earth system. Conservation of TE in this context refers to having a closed
 26 TE budget. For example, the TE change in a column in the atmosphere is exactly balanced
 27 by the net sources/sinks given by the fluxes through the column. The fluxes into the at-
 28 mospheric component from the surface models must be balanced by the fluxes in the re-
 29 spective surface components and so on. Henceforth we will focus only on the atmospheric
 30 component which, in a numerical model, is split into a resolved-scale component (the dy-
 31 namical core) and a sub-grid-scale component (parameterizations or, in modeling jargon,
 32 physics). While there have been many studies on energy flow in the Earth system through
 33 analysis of re-analysis data and observations [Trenberth and Fasullo, 2018, and references
 34 herein], there has been less focus on spurious TE sources/sinks in numerical models.

35 The atmospheric equations of motion conserve TE but the discretizations used in cli-
 36 mate and weather models are usually not inherently TE conservative. Exact conservation
 37 is probably not necessary but conservation to within $\sim 0.01 \text{ W/m}^2$ has been considered
 38 sufficient to avoid spurious trends in century long simulations [Boville, 2000; Williamson
 39 *et al.*, 2015]. Spurious sources and sinks of TE can be introduced by the dynamical core,
 40 physics, physics-dynamics coupling as well as discrepancies between the TE of the con-
 41 tinuous and discrete equations of motion and for the physics. Hence the study of TE con-
 42 servation in comprehensive models of the atmosphere quickly becomes a quite complex
 43 and detailed matter. In addition there can easily be compensating errors in the system as a
 44 whole.

45 Here we focus on versions of the Community Atmosphere Model (CAM) that use
 46 the spectral-element [SE, Lauritzen *et al.*, 2018] and finite-volume [FV, Lin, 2004] dy-
 47 namical cores. These dynamical cores couple with physics in a time-split manner, i.e.
 48 physics receives a state updated by dynamics [see Williamson, 2002, for a discussion
 49 of time-split versus process split physics-dynamics coupling in the context of CAM]. In
 50 its pure time-split form the physics tendencies are added to the state previously produced
 51 by the dynamical core and the resulting state provides the initial state for the subsequent
 52 dynamical core calculation. We refer to this as *state-updating* (`ftype=1` in CAM code).
 53 Alternatively, when the dynamical core adopts a shorter time step than the physics, say
 54 `nsplit` sub-steps, then $(1/\text{nsplit})$ th of the physics-calculated tendency is added to the
 55 state before each dynamics sub-step. We refer to this modification of time-splitting as
 56 *dribbling* (`ftype=0`). CAM-FV uses the *state-update* (`ftype=1`) approach while CAM-SE
 57 has options to use *state-update* (`ftype=1`), *dribbling* (`ftype=0`) or a combination of the
 58 two i.e. mass-variables use *state-updating* and remaining variables use *dribbling*. We refer
 59 to this as *combination* (`ftype=2`). The *dribbling* variants can lead to spurious sources or
 60 sinks of TE (and mass) referred to here as physics-dynamics coupling errors.

61 The dynamical core usually has inherent or specified filters to control spurious noise
 62 near the grid scale which will lead to energy dissipation [Thuburn, 2008; Jablonowski

and Williamson, 2011]. Similarly models often have sponge layers to control the solution near the top of the model that may be a sink of TE. There are examples of numerical discretizations of the adiabatic frictionless equations motion that are designed so that TE is conserved in the absence of time-truncation and filtering errors [e.g., Eldred and Randall, 2017; McRae and Cotter, 2013], e.g., mimetic spectral-element discretizations such as the one used in the horizontal in CAM-SE [Taylor, 2011]. These provide consistency between the discrete momentum and thermodynamic equations leading to global conservation associated with the conversion of potential to kinetic energy. In spectral transform models it is customary to add the energy change due to explicit diffusion on momentum back as heating (referred to as frictional heating), so that the diffusion of momentum does not affect the TE budget [see, e.g., p.71 in Neale et al., 2012]. This is also done in CAM-SE [Lauritzen et al., 2018].

The purpose of this paper is to provide a detailed global TE analysis of CAM. We assess TE errors due to various steps in the model algorithms. The paper is outlined as follows. In section 2 the continuous TE formulas are given and a detailed description of spurious TE sources/sinks that can occur in a model as a whole, and the associated diagnostics used to perform the TE analysis, are defined. In section 3 the model is run in various configurations to assess their effects on TE conservation. This includes various physics-dynamics coupling experiments leading to a rather detailed discussion of mass budget closure. We also investigate the effect of using a limiter in the vertical remapping of momentum, assess energy discrepancy errors and impacts on TE of simplifying surface conditions and dry atmosphere experiments. The paper ends with conclusions.

2 Method

2.1 Defining total energy (TE)

In the following it is assumed that the model top and bottom are coordinate surfaces and that there is no flux of mass through the model top and bottom. In a dry hydrostatic atmosphere the TE equation integrated over the entire sphere is given by

$$\frac{d}{dt} \int_{z=z_s}^{z=z_{top}} \iint_S E_v \rho^{(d)} dA dz = \int_{z=z_s}^{z=z_{top}} \iint_S F_{net} \rho^{(d)} dA dz, \quad (1)$$

[e.g., Kasahara, 1974] where F_{net} is net flux calculated by the parameterizations (e.g., heating and momentum forcing), d/dt the total/material derivative, z_s is the height of the surface, S the sphere, $\rho^{(d)}$ the density of dry air, E_v is the TE and dA is an infinitesimal area on the sphere. E_v can be split into kinetic energy $K = \frac{1}{2}\mathbf{v}^2$ (\mathbf{v} is the wind vector), internal energy $c_v^{(d)}T$, where $c_v^{(d)}$ is the heat capacity of dry air at constant volume, and potential energy $\Phi = gz$

$$E_v = K + c_v^{(d)}T + \Phi. \quad (2)$$

If the vertical integral is performed in a mass-based vertical coordinate, e.g., pressure, then the integrated TE equation for a dry atmosphere can be written as

$$\frac{d}{dt} \int_{p=p_s}^{p=p_{top}} \iint_S E_p \rho^{(d)} dA dp + \frac{d}{dt} \iint_S \Phi_s p_s dA = \int_{p=p_s}^{p=p_{top}} \iint_S F_{net} \rho dA dp, \quad (3)$$

[e.g., Kasahara, 1974] where

$$E_p = K + c_p^{(d)}T. \quad (4)$$

In a moist atmosphere, however, there are several definitions of TE used in the literature related to what heat capacity is used for water vapor and whether or not condensates are accounted for in the energy equation. To explain the details of that we focus on the energy equation for CAM-SE.

CAM-SE is formulated using a terrain-following hybrid-sigma vertical coordinate η but the coordinate levels are defined in terms of dry air mass per unit area ($M^{(d)}$) instead of total air mass; $\eta^{(d)}$ [see Lauritzen et al., 2018, for details]. In such a coordinate

106 system it is convenient to define the tracer state in terms of a dry mixing ratio instead of
 107 moist mixing ratio

$$m^{(\ell)} \equiv \frac{\rho^{(\ell)}}{\rho^{(d)}}, \text{ where } \ell = 'wv', 'cl', 'ci', 'rn', 'sw', \quad (5)$$

108 where $\rho^{(d)}$ is the mass of dry air per unit volume of moist air and $\rho^{(\ell)}$ is the mass of the
 109 water substance of type ℓ per unit volume of moist air. Moist air refers to air containing
 110 dry air ('d'), water vapor ('wv'), cloud liquid ('cl'), cloud ice ('ci'), rain amount ('rn')
 111 and snow amount ('sw'). For notational purposes define the set of all components of air

$$\mathcal{L}_{all} = \{'d', 'wv', 'cl', 'ci', 'rn', 'sw'\}, \quad (6)$$

112 Define associated heat capacities at constant pressure $c_p^{(\ell)}$. We refer to condensates as being
 113 *thermodynamically and inertially active* if they are included in the thermodynamic
 114 equation and momentum equations. E.g. if the thermodynamic equation is formulated
 115 in terms of temperature the energy conversion term includes a generalized heat capacity
 116 which is a function of the condensates and their associated heat capacities [see, e.g., sec-
 117 tion 2.3 in *Lauritzen et al., 2018*]. Similarly the weight of the condensates is included in
 118 the pressure field and pressure gradient force. How many and which condensates are ther-
 119 modynamically/inertially active in the dynamical core is controlled with namelist `qsize_condensate_loading`.
 120 If `qsize_condensate_loading=1` only water vapor ('wv') is active, `qsize_condensate_loading=3`
 121 'wv', 'cl', and 'ci' are active, and if `qsize_condensate_loading=5` then 'wv', 'cl', 'ci', 'rn',
 122 and 'sw' are included.

123 Using the $\eta^{(d)}$ vertical coordinate and dry mixing ratios the TE (per unit area) that
 124 the frictionless adiabatic equations of motion in the CAM-SE dynamical core conserves is

$$\widehat{E}_{dyn} = \frac{1}{\Delta S} \int_{\eta=0}^{\eta=1} \iint_S \left(\frac{1}{g} \frac{\partial M^{(d)}}{\partial \eta^{(d)}} \right) \sum_{\ell \in \mathcal{L}_{all}} \left[m^{(\ell)} \left(K + c_p^{(\ell)} T + \Phi_s \right) \right] dA d\eta^{(d)}, \quad (7)$$

125 where ΔS is the surface area of the sphere, Φ_s is the surface geopotential and (\cdot) refers to
 126 the global average.

127 In the CAM physical parameterizations a different definition of TE is used. Due to
 128 the evolutionary nature of the model development, the parameterizations have not yet been
 129 converted to match the SE dynamical core. For the computation of TE, condensates are
 130 assumed to be zero and the heat capacity of moisture is the same as for dry air. This is
 131 equivalent to using a moist mass (dry air plus water vapor) but c_p of dry air:

$$\widehat{E}_{phys} = \frac{1}{\Delta S} \int_{\eta=0}^{\eta=1} \iint_S \left(\frac{1}{g} \frac{\partial M^{(d)}}{\partial \eta^{(d)}} \right) \left(1 + m^{(wv)} \right) \left[\left(K + c_p^{(d)} T + \Phi_s \right) \right] dA d\eta^{(d)}. \quad (8)$$

132 We note that earlier versions of CAM using the spectral transform dynamical core used
 133 c_p of moist air. The adiabatic, frictionless equations of motion in the CAM-SE dynamical
 134 core can be made consistent with E_{phys} by not including condensates in the mass/pressure
 135 field as well as energy conversion term in the thermodynamic equation and setting the
 136 heat capacity for moisture to $c_p^{(d)}$ [Taylor, 2011]. We refer to this version of CAM-SE as
 137 the *energy consistent* version.

138 2.2 Spurious energy sources and sinks

139 In a weather/climate model TE conservation errors can appear in many places through-
 140 out the algorithm. Below is a general list of where conservation errors can appear with
 141 specific examples from CAM:

- 142 1. *Parameterization errors*: Individual parameterizations may not have a closed en-
 143 ergy budget. CAM parameterizations are required to have a closed energy budget
 144 under the assumption that pressure remains constant during the computation of the

- 145 subgrid-scale parameterization tendencies. In other words, the TE change in the
 146 column is exactly balanced by the net sources/sinks given by the fluxes through the
 147 column.
- 148 2. *Pressure work error*: That said, if parameterizations update specific humidity then
 149 the surface pressure changes (e.g., moisture entering or leaving the column). In
 150 that case the pressure changes which, in turn, changes TE. This is referred to as
 151 *pressure work error* [section 3.1.8 in *Neale et al.*, 2012].
- 152 3. *Continuous TE formula discrepancy*: If the continuous equations of motion for the
 153 dynamical core conserve a TE different from the one used in the parameterizations
 154 then an energy inconsistency is present in the system as a whole. This is the case
 155 with the new version of CAM-SE that conserves a TE that is more accurate and
 156 comprehensive than that used in the CAM physics package as discussed above. As
 157 also noted above, this mismatch arose from the evolutionary nature of the model
 158 development and not by deliberate design; and should be eliminated in the future.
- 159 4. *Dynamical core errors*: [mention that we assume that dynamical core is inherently
 160 mass conservative] Energy conservation errors in the dynamical core, not related to
 161 physics-dynamics coupling errors, can arise in multiple parts of the algorithms used
 162 to solve the equations of motion. For dynamical cores employing filtering [e.g.,
 163 limiters in flux operators *Lin*, 2004] and/or possessing inherent damping which
 164 controls small scales, it is hard to isolate their energy dissipation from other errors
 165 in the discretization. If a hyperviscosity term or some other diffusion is added to
 166 the momentum equation, then one can diagnose the local energy dissipation from
 167 such damping and add a corresponding heating to balance it (frictional heating).
 168 There may also be energy loss from viscosity applied to other variables such a tem-
 169 perature or pressure which is harder to compensate. Here is a break-down relevant
 170 to CAM-SE using a floating Lagrangian vertical coordinate:
- 171 • Horizontal inviscid dynamics: Energy errors resulting from solving the inviscid,
 172 adiabatic equations of motion.
- 173 • Hyperviscosity: Filtering errors.
- 174 • Vertical remapping: The vertical remapping algorithm from Lagrangian to Eule-
 175 rian reference surfaces does not conserve TE.
- 176 • Near round-off negative values of water vapor which are filled to a minimal
 177 value without compensation.

178 If a dynamical core is not inherently mass-conservative with respect to dry air, wa-
 179 ter vapor and condensates then TE conservation is affected since

$$\int_{\eta=0}^{\eta=1} \iint_S \left(\frac{1}{g} \frac{\partial M^{(d)}}{\partial \eta^{(d)}} \right) \sum_{\ell \in \mathcal{L}_{all}} \left[m^{(\ell)} \right] dA d\eta^{(d)} \quad (9)$$

- 180 is not conserved. Henceforth we assume that the dynamical core is based on an
 181 inherently mass-conservative formulation which is the case for CAM-SE and CAM-
 182 FV.
- 183 5. *Physics-dynamics coupling (PDC)*: Assume that physics computes a tendency. Usu-
 184 ally the tendency (forcing) is passed to the dynamical core which is responsible for
 185 adding the tendencies to the state. PDC energy errors can be split into three types:

- 186 • ‘Dribbling’ errors (or, equivalently, temporal PDC errors): If the TE increment
 187 from the parameterizations does not match the change in TE when the tenden-
 188 cies are added to the state in the dynamical core, then there will be a spurious
 189 PDC error. This will not happen with the *state-update* approach in which the
 190 tendencies are added immediately after physics and before the dynamical core
 191 advances the solution in time.

192 PDC errors in temperature tendencies occur because the *T*-increment (call it
 193 ΔT) that the parameterizations prescribe leads to a dry thermal energy change of
 194 $\Delta M^{(d)} \Delta T$ which will not match the equivalent dry thermal energy change when

the temperature tendency is added in smaller chunks in the dynamical core during the ‘dribbling’ of ΔT . The discrepancy occurs because $\Delta M^{(d)}$ changes during each dynamics time-step and hence the thermal energy change due to physics forcing accumulated during the ‘dribbling’ will not equal $\Delta M^{(d)}\Delta T$. This error could possibly be eliminated by using thermal energy forcing instead of temperature increments. Similarly, PDC errors in velocity component forcing increments ($\Delta u, \Delta v$) occur because the dry kinetic energy change of $\Delta M^{(d)} [(\Delta u)^2 + (\Delta v)^2]$ will not match the equivalent dry kinetic energy change when ‘dribbling’ velocity component forcing increments ($\Delta u, \Delta v$). It is less clear how to eliminate this error as kinetic energy is a quadratic quantity.

A different PDC error can occur when mass-variable tendencies such as vapor vapor forcing, cloud liquid, etc. are ‘dribbled’ during the dynamical core integration. This can lead to a spurious source if there is logic in the dynamical core preventing mixing ratios to become negative. This is referred to as ‘clipping’ PDC errors and are described/discussed in detail in Section 3.2.1.

- *Change of vertical grid/coordinate errors:* If the vertical coordinates in physics and in the dynamical core are different then there can be spurious PDC energy errors even when using the state-update method for adding tendencies to the dynamical core state. For example, many non-hydrostatic dynamical cores [e.g. Skamarock *et al.*, 2012] use a terrain-following height coordinate whereas physics uses pressure.
 - *Change of horizontal grid errors:* If the physics tendencies are computed on a different horizontal grid than the dynamical core then there can be spurious energy errors from mapping tendencies and/or variables between horizontal grids [e.g., Herrington *et al.*, 2018].
6. *Compensating Energy fixers:* To avoid TE conservation errors which could accumulate and ultimately lead to a climate drift, it is customary to apply an arbitrary energy fixer to restore TE conservation. Since the spatial distribution of many energy errors, in general, is not known, global fixers are used. In CAM a uniform increment is added to the temperature field to compensate for TE imbalance from all processes, i.e. dynamical core, physics-dynamics coupling, TE formula discrepancy, energy change due to pressure work **error**, and possibly parameterization errors if present.

2.3 Diagnostics

The discrete global averages ($\widehat{\cdot}$) are computed consistent with the discrete model grid as outlined in section 2.2. of Lauritzen *et al.* [2014]. The TE global average tendency is denoted

$$\partial \widehat{E} \equiv \frac{d\widehat{E}}{dt}. \quad (10)$$

By computing the global TE averages \widehat{E} at appropriate places in the model algorithms, we can directly compute $\partial \widehat{E}$ due to various processes (such as viscosity, vertical remapping, physics-dynamics coupling, pressure work **error**, etc.) by differencing \widehat{E} from after and before the algorithm takes place. This has been implemented using CAM history infrastructure by computing column integrals of energy at various places in CAM and outputting the 2D energy fields. CAM history internally handles accumulation and averaging in time at each horizontal grid point. The global averages are computed externally from the grid point vertical integrals on the history files (stored in double precision). The places in CAM where we compute/capture the grid point vertical integral E are named using three letters where the first letter refers to whether the vertical integral is performed in physics ('p') or in the dynamical core ('d'). The trailing two letters refer to the specific location in dynamics or physics. For example, 'BP' refers to 'Before Physics' and 'AP' to 'After Physics'; the associated total energies are denoted E_{pBP} and E_{pAP} , respectively.

The TE tendency from the parameterizations is the difference between E_{pBP} and E_{pAP} divided by the time-step. The terms and tendencies are then averaged globally externally to the model. The pseudo-code in Figure 1 defines the acronyms in terms of where in the CAM-SE algorithm the TE vertical integrals are computed and output. For details on the CAM-SE algorithm please see *Lauritzen et al.* [2018].

Before defining the individual terms in detail we briefly review the model time stepping sequence starting with the physics component as illustrated in Figure 1. The energy fixer is applied first to compensate for the spurious net energy change from all components introduced during the previous time step. We will describe this in more detail after the various sources and sinks are elucidated. The parameterizations are applied next and are required to be energy conserving. They update the state and accumulate the total physics tendency (forcing). At this stage the state is saved for use in the energy fixer in the next time step. Any changes in the global average energy after this are spurious and are compensated by the fixer. The parameterizations update the water vapor but not the moist pressure, implying a non-physical change in the dry mass of the atmosphere. The dry mass correction corrects the dry mass back to its proper value.

The forcing (physics tendency) from the parameterizations is passed to the dynamical core. If the physics and dynamics operate on different grids, the forcing is remapped here. The dynamics operates on a shorter time step than the physics and is sub-stepped. The remapped forcing is applied to the dynamics state, saved from the end of the previous dynamics step, using either *state-updating*, *dribbling*, or *combination* as described in the introduction. The dynamics then advances the adiabatic frictionless flow in the floating Lagrangian layers over a further set of sub-steps. Hyperviscosity is applied next with further sub-stepping required for computational stability of the explicit discrete approximations. The energy loss from the specified momentum viscosity is calculated locally and is balanced by adding a local change to the temperature, referred to as *frictional heating*. This set of dynamics sub-steps is followed by the vertical remapping from Lagrangian to Eulerian reference layers. The remapping is required to provide layers consistent with the parameterization formulations. The vertical remapping sub-steps are required for stability if the Lagrangian layers become too thin.

At the end of the dynamics, the state is saved to be used by the dynamics the next time step and is also passed to the physics, with a remapping if the dynamics and physics grids differ. At the beginning of the physics the difference in energy between this state and the state saved after the physics during the previous time step is the amount needed to be added or subtracted by the energy fixer. It represents the accumulation of all spurious sources from the dry mass correction, remappings between physics and dynamics grids (if applicable), dynamical core, differing energy definitions (if present), hyperviscosity, and vertical remapping.

We now define the following energy tendencies corresponding to the itemized list in section 2.2 with references to terms indicated in Figure 1. We start just after the energy fixer which will be defined at the end.

1. $\partial\widehat{E}^{(param)}$: TE tendency due to parameterizations. In CAM the TE budget for each parameterization is closed (assuming pressure is unchanged) so $\partial\widehat{E}^{(param)}$ is balanced by net fluxes in/out of the physics columns. Note that this is the only energy tendency that is not spurious since CAM parameterizations have a closed TE budget. This TE tendency is discretely computed as

$$\partial\widehat{E}_{phys}^{(param)} = \frac{\widehat{E}_{pAP} - \widehat{E}_{pBP}}{\Delta t_{phys}}, \quad (11)$$

where Δt_{phys} is the physics time-step (default 1800s) and the subscript *phys* on $\partial\widehat{E}$ refers to the energy tendency computed in CAM physics.

301 2. $\partial\widehat{E}^{(pwork)}$: Total spurious energy tendency due to pressure work **error**

$$\partial\widehat{E}_{phys}^{(pwork)} = \frac{\widehat{E}_{pAM} - \widehat{E}_{pAP}}{\Delta t_{phys}}. \quad (12)$$

302 Since CAM-SE dynamical core is based on a dry-mass vertical coordinate the pres-
 303 sure work **error** takes place implicitly in the dynamical core. But the TE tendency
 304 due to pressure work **error** is conveniently computed in physics since dynamical
 305 cores based on a moist vertical coordinate (e.g., CAM-FV) require pressure and
 306 moist mixing ratios to be adjusted for dry mass conservation and tracer mass con-
 307 servation [section 3.1.8 in *Neale et al.*, 2012]. The difference of TE after and be-
 308 fore this adjustment is the TE tendency due to pressure work **error**. In a dry mass
 309 vertical coordinate based on dry mixing ratios neither dry mass layer thickness nor
 310 dry mixing ratios need to be adjusted to take into account moisture changes in the
 311 column. For labeling purposes, the 'total forcing' associated with physics (at least
 312 in CAM) consists of parameterizations, pressure work **error** and TE fixer, although
 313 strictly speaking the fixer includes components from the dynamics as will be seen.

$$\partial\widehat{E}_{phys}^{(phys)} \equiv \partial\widehat{E}_{phys}^{(param)} + \partial\widehat{E}_{phys}^{(pwork)} + \partial\widehat{E}_{phys}^{(efix)} = \frac{\widehat{E}_{pAM} - \widehat{E}_{pBF}}{\Delta t_{phys}}. \quad (13)$$

314 where the energy fixer TE tendency is

$$\partial\widehat{E}_{phys}^{(efix)} = \frac{\widehat{E}_{pBP} - \widehat{E}_{pBF}}{\Delta t_{phys}}. \quad (14)$$

315 After all the TE budget terms have been defined, the exact composition of $\partial\widehat{E}_{phys}^{(efix)}$
 316 will be presented.

- 317 3. $\partial\widehat{E}^{(discr)}$: If the physics uses a TE definition different from the TE that the con-
 318 tinuous equations of motion in the dynamical core conserve (i.e. in the absence of
 319 discretization errors), then there is a TE discrepancy tendency. This complicates
 320 the energy analysis as one can not compare TE computed in physics \widehat{E}_{phys} directly
 321 with TE computed in the dynamical core \widehat{E}_{dyn} . This makes errors associated with
 322 this discrepancy tricky to assess. That said, the TE tendencies computed using the
 323 dynamical core TE formula $\partial\widehat{E}_{dyn}$ are well defined (self consistent) and similarly
 324 for TE tendencies computed using the 'physics formula' for TE, $\partial\widehat{E}_{phys}$.
- 325 4. The TE tendency from the dynamical core is split into several terms: Horizontal
 326 adiabatic dynamics (dynamics excluding physics forcing tendency)

$$\partial\widehat{E}_{dyn}^{(2D)} = \frac{\widehat{E}_{dAD} - \widehat{E}_{dBBD}}{\Delta t_{dyn}}, \quad (15)$$

327 where over a single dynamics sub-step $\Delta t_{dyn} = \frac{\Delta t_{phys}}{\text{nsplit}\times\text{rsplit}}$ (the loop bounds
 328 `nsplit`, `rsplit`, etc. are explained in Figure 1).

329 In CAM-SE the viscosity is explicit so one can compute the TE tendency due to
 330 hyperviscosity and its associated frictional heating

$$\partial\widehat{E}_{dyn}^{(hvvis)} = \frac{\widehat{E}_{dAH} - \widehat{E}_{dBH}}{\Delta t_{hvvis}}, \quad (16)$$

331 which, in CAM-SE, includes a frictional heating term from viscosity on momentum

$$\partial\widehat{E}_{dyn}^{(fheat)} = \frac{\widehat{E}_{dAH} - \widehat{E}_{dCH}}{\Delta t_{hvvis}}, \quad (17)$$

332 where $\Delta t_{hvvis} = \frac{\Delta t_{phys}}{\text{nsplit}\times\text{rsplit}\times\text{hypervis_subcycle}}$ is the time step of the sub-stepped
 333 viscosity. The residual

$$\partial\widehat{E}_{dyn}^{(res)} = \partial\widehat{E}_{dyn}^{(2D)} - \partial\widehat{E}_{dyn}^{(hvvis)}, \quad (18)$$

334 is the energy error due to inviscid dynamics and time-truncation errors.

335 The energy tendency due to vertical remapping is

$$\partial \widehat{E}_{dyn}^{(remap)} = \frac{\widehat{E}_{dAR} - \widehat{E}_{dAD}}{\Delta t_{remap}}, \quad (19)$$

336 where $\Delta t_{remap} = \frac{\Delta t_{phys}}{n_{split}}$.

337 The 3D adiabatic dynamical core (no physics forcing but including friction) energy
338 tendency is denoted

$$\partial \widehat{E}_{dyn}^{(adiab)} = \partial \widehat{E}_{dyn}^{(2D)} + \partial \widehat{E}_{dyn}^{(remap)}. \quad (20)$$

339 5. $\partial \widehat{E}^{(pdc)}$: Total spurious energy tendency due to physics-dynamics coupling errors is
340 the difference between the energy tendency from physics and the energy tendency
341 in the dynamics resulting from adding the physics increment to the dynamical core
342 state

$$\partial \widehat{E}_{phys}^{(pdc)} = \partial \widehat{E}_{phys}^{(phys)} - \partial \widehat{E}_{dyn}^{(phys)} \text{ assuming } \partial \widehat{E}^{(discr)} = 0, \quad (21)$$

343 where

$$\partial \widehat{E}_{dyn}^{(phys)} = \frac{\widehat{E}_{dB} - \widehat{E}_{dA}}{\Delta t_{pdc}}, \quad (22)$$

344 and Δt_{pdc} is the time-step between physics increments being added to the dynami-
345 cal core. Remember we are dealing with average rates so terms computed with dif-
346 ferent time steps can be compared, but differences cannot be taken between terms
347 sampled with different time steps.

348 The physics-dynamics coupling TE tendency $\partial \widehat{E}^{(pdc)}$ makes use of TE formulas
349 in dynamics and in physics so (21) is only well-defined if the TE formula discrep-
350 ency is zero, $\partial \widehat{E}^{(discr)} = 0$. As mentioned in Section 2.1, CAM-SE has the op-
351 tion to switch the continuous equations of motion conserving the TE used by CAM
352 physics (8) instead of the more comprehensive TE formula (7).

353 In CAM-SE there are 3 physics-dynamics coupling algorithms described in detail
354 in section 3.6 in *Lauritzen et al. [2018]* and reviewed in the introduction here. One
355 is *state-update* in which the entire physics increments are added to the dynamics
356 state at the beginning of dynamics (referred to as *ftype=1*), in which case $\Delta t_{pdc} =$
357 Δt_{phys} . Another is *dribbling* in which the physics tendency is split into *nsplit*
358 equal chunks and added throughout dynamics (more precisely after every vertical
359 remapping; referred to as *ftype=0* resulting in $\Delta t_{pdc} = \frac{1}{n_{split}} \Delta t_{phys}$), and then a
360 *combination* of the two (referred to as *ftype=2*) where tracers (mass variables) use
361 *state-update* (*ftype=1*) and all other physics tendencies use *dribbling* (*ftype=0*).

362 6. $\partial \widehat{E}^{(efix)}$: Global energy fixer tendency, defined in (14), is applied at the beginning
363 of the parameterizations. The correction needed is the global average difference
364 between the state passed from the dynamics and the state that was saved after the
365 physics updated the state but before the dry mass correction. It includes all spu-
366 rious sources from the dry mass correction, remappings between physics and dy-
367 namics, dynamical core, differing energy definitions (if present), hyperviscosity, and
368 vertical remapping.

369 2.4 A few observations regarding the energy budget terms

370 It is useful to note that the energy fixer ‘fixes’ energy errors for the dynamical core,
371 pressure work **error**, physics-dynamics coupling and TE discrepancy

$$-\partial \widehat{E}_{phys}^{(efix)} = \partial \widehat{E}_{phys}^{(pwork)} + \partial \widehat{E}_{dyn}^{(adiab)} + \partial \widehat{E}^{(pdc)} + \partial \widehat{E}^{(discr)}. \quad (23)$$

372 The forcing from the parameterizations, $\partial \widehat{E}_{phys}^{(param)}$, does not appear in this budget (al-
373 though the dynamical core state does ‘feel’ the parameterization forcing) as the energy
374 cycle for the parameterizations is, by design in CAM, closed (balanced by fluxes in/out of

375 the physics columns). If $\partial\widehat{E}^{(discr)} = 0$, one can use (23) to diagnose energy dissipation
 376 in the dynamical core and physics-dynamics coupling from quantities computed only in
 377 physics

$$\partial\widehat{E}_{dyn}^{(adiab)} + \partial\widehat{E}^{(pdc)} = -\partial\widehat{E}_{phys}^{(efix)} - \partial\widehat{E}_{phys}^{(pwork)} \text{ for } \partial\widehat{E}^{(discr)} = 0. \quad (24)$$

378 This is useful if the diagnostics are not implemented in the dynamical core; in particular,
 379 if the *state-update* (`ftype=1`) physics-dynamics coupling method is used then $\partial\widehat{E}^{(pdc)} = 0$
 380 and the TE errors in the dynamical core can be computed without diagnostics imple-
 381 mented in the dynamical core. Also, (24) provides an alternative formula for $\partial\widehat{E}^{(pdc)}$
 382 compared to (21):

$$\partial\widehat{E}^{(pdc)} = -\partial\widehat{E}_{phys}^{(efix)} - \partial\widehat{E}_{phys}^{(pwork)} - \partial\widehat{E}_{dyn}^{(adiab)} \text{ assuming } \partial\widehat{E}^{(discr)} = 0. \quad (25)$$

383 If $\partial\widehat{E}^{(pdc)} = 0$ (23) can be used to compute $\partial\widehat{E}^{(discr)}$

$$\partial\widehat{E}^{(discr)} = -\partial\widehat{E}_{phys}^{(efix)} - \partial\widehat{E}_{phys}^{(pwork)} - \partial\widehat{E}_{dyn}^{(adiab)}, \text{ assuming } \partial\widehat{E}^{(pdc)} = 0. \quad (26)$$

384 Note that we can not use (21) to compute $\partial\widehat{E}^{(discr)}$ since $\widehat{E}_{phys} \neq \widehat{E}_{dyn}$.

3 Results

386 A series of simulations have been performed with CESM2.1 using CAM version 6
 387 (CAM6) physics (<https://doi.org/10.5065/D67H1H0V>) on NCAR's Cheyenne cluster
 388 [*Computational and Information Systems Laboratory*, 2017]. All simulations are at nom-
 389 inally $\sim 1^\circ$ horizontal resolution (for CAM-SE that is 30×30 elements on each cubed-
 390 sphere face and for CAM-FV its 192×288 latitudes-longitudes) and using the standard
 391 32 levels in the vertical. Unless otherwise noted all simulations are 13 months in dura-
 392 tion and the last 12 months are used in the analysis. Total energy budgets are summarized
 393 in Table 1 and discussed below. The first column gives identifying ‘Descriptors’ which
 394 are briefly summarized below and defined in more detail in the following sections. The
 395 section titles also include the ‘Descriptor’ from Table 1 to make it easier for the reader
 396 to match Table entries with discussion in the text. Important changes to TE errors are
 397 marked with bold font in Table 1.

398 Various configurations are used and referred to in terms of the *COMPSET* (Com-
 399 ponent Set) value used in CESM2.1. The *COMPSET F2000climo* configuration refers
 400 to ‘real-world’ AMIP (Atmospheric Model Intercomparison Project) type simulations us-
 401 ing perpetual year 2000 SST (Sea Surface Temperature) boundary conditions. The first 7
 402 simulations in the table (those above the horizontal line) are such AMIP-type simulations
 403 (*F2000climo*) with the first serving as a control for the 6 following variants. The remain-
 404 ing 5 simulation descriptors (below the horizontal line in Table 1) list their *COMPSET* or
 405 dynamical core settings.

- 406 • *TE consistent*: The TE consistent version uses *state update* physics-dynamics cou-
 407 pling (`ftype 1`) described in section 3.1,
- 408 • ‘*dribbling*’ A: as *TE consistent* but with *dribbling* physics-dynamics coupling (`ftype`
 409 `0`) (section 3.2),
- 410 • ‘*dribbling*’ B: as *TE consistent* but with *dribbling* combination physics-dynamics
 411 coupling (`ftype 2`) (section 3.2),
- 412 • *vert limiter*: as *TE consistent* but using limiters in the vertical remapping of mo-
 413 mentum (section 3.3),
- 414 • *smooth topo*: as *TE consistent* but using smoother topography (see section 3.4),
- 415 • *energy discr*: The version with energy discrepancy (but no physics-dynamics cou-
 416 pling errors) described in section 3.5,
- 417 • *default*: as *energy discr* version but with `ftype=2` which is the current default
 418 CAM-SE (section 3.5),

Table 1. TE tendencies in units of W/m^2 associated with various aspects of CAM-SE run in AMIP-type setup (unless otherwise noted). Column 1 is the identifier for the model configuration. See the text for a brief summary of these descriptors. They are defined in more detail in the following sections where the section titles also include the ‘Descriptor’ from Table 1 to make it easier for the reader to match Table entries with discussion in the text. Column 2 is $N = \text{qsize_condensate_loading}$ identifying how many water species are thermodynamically/**inertially** active in the dynamical core (see section 2.1 for details). Column 3, lcp_moist , indicates whether or not the heat capacity includes water variables or not and column 4 shows physics-dynamics coupling method $f\text{type}$. The TE tendencies $\partial \widehat{E}$ in columns 5-14 are defined in section 2.3. If $\partial \widehat{E}$ is less than $10^{-5} W/m^2$ it is set to zero in the Table. Significant changes compared to the baseline (*TE consistent* configuration) discussed in the main text are in bold font.

Descriptor	N	lcp_moist	$f\text{type}$	$\partial \widehat{E}_{\text{phys}}^{(p\text{work})}$	$\partial \widehat{E}_{\text{phys}}^{(efix)}$	$\partial \widehat{E}_{\text{phys}}^{(discr)}$	$\partial \widehat{E}_{\text{dyn}}^{(2D)}$	$\partial \widehat{E}_{\text{dyn}}^{(heat)}$	$\partial \widehat{E}_{\text{dyn}}^{(vis)}$	$\partial \widehat{E}_{\text{dyn}}^{(res)}$	$\partial \widehat{E}_{\text{dyn}}^{(remap)}$	$\partial \widehat{E}_{\text{dyn}}^{(adiab)}$	$\partial \widehat{E}_{\text{dyn}}^{(pdc)}$
<i>TE consistent</i>	1	false	1	0.312	0.300	0	-0.601	-0.608	0.565	0.007	-0.011	-0.613	0
‘dribbling’ <i>A</i>	1	false	0	0.315	0.313	0	-0.577	-0.584	0.568	0.007	-0.011	-0.588	0.469
‘dribbling’ <i>B</i>	1	false	2	0.316	0.341	0	-0.598	-0.606	0.563	0.008	-0.011	-0.609	0.484
<i>vert limiter</i>	1	false	1	0.317	0.472	0	-0.590	-0.597	0.509	0.006	-0.199	-0.789	0
<i>smooth topo</i>	1	false	1	0.315	-0.008	0	-0.295	-0.300	0.493	0.005	-0.012	-0.307	0
<i>energy discr</i>	5	true	1	0.332	-0.313	0.594	-0.603	-0.612	0.575	0.009	-0.011	-0.614	-
<i>default</i>	5	true	2	0.316	-0.272	-0.578	-0.587	-0.579	0.579	0.010	-0.012	-0.589	-
<i>QPC6</i>	1	false	1	0.305	-0.169	0	-0.129	-0.131	0.477	0.001	-0.007	-0.136	0
<i>FHS94</i>	1	false	2	-	-	-0.025	-0.025	0.122	0	0.005	-0.020	-	-
<i>FV</i>	1	false	1	0.304	0.670	0	-	-	-	-	-0.974	0	-
<i>CSLAM</i>	1	false	1	0.312	0.239	0	-0.547	-0.557	0.620	0.010	-0.011	-0.558	-0.070
<i>CSLAM default</i>	5	true	2	0.320	-0.342	-	-0.524	-0.537	0.641	0.013	-0.011	-0.535	-

- *QPC6*: A simplified aqua-planet setup based on the *TE consistent*, i.e an aqua-planet setup using CAM6 physics; an ocean covered planet in perpetual equinox, with fixed, zonally symmetric sea surface temperatures [Neale and Hoskins, 2000; Medeiros et al., 2016] (section 3.6),
- *FSH94*: Dry dynamical core configuration based on Held-Suarez forcing which relaxes temperature to a zonally symmetric equilibrium temperature profile and simple linear drag at the lower boundary [Held and Suarez, 1994] (section 3.7),,
- *FV*: A configuration with the SE dynamical core replaced with the finite-volume core (section 3.8), and
- *CSLM*: The quasi equal-area physics grid configuration of CAM-SE based on the TE consistent setup (section 3.9)
- *CSLM default*: Same as *CSLM* configuration but with `ftype=2` and all forms of water thermodynamically/**inertially** active in the dynamical core.

438 3.1 *TE consistent: state-update physics-dynamics coupling (ftype=1) and no TE 439 formula discrepancy*

440 This configuration is the most energetically consistent in that the physical parametrizations and the continuous equations of motion on which the dynamical core is based,
441 conserve the same TE (defined in equation (8)); and there are no spurious sources/sinks in
442 physics-dynamics coupling. Energetic consistency in dynamics and physics is obtained
443 by setting $c_p^{(\ell)} \equiv c_p^d$ and $\mathcal{L}_{all} = \{‘d’, ‘wv’\}$ in the dynamical core equations of motion
444 and TE computations. Associated namelist changes resulting in this configuration are
445 `lcp_moist = .false., se_qsize_condensate_loading = 1`, and `ftype = 1`.

446 The TE consistent configuration in AMIP-type simulation (*F2000climo*) is used to
447 compute baseline TE tendencies which will be used to compare with other model configura-
448 tions. First we establish how long an average is needed to get robust TE tendency
449 estimates. Figure 2 shows $\partial\widehat{E}$ for various aspects of CAM-SE as a function of time. The
450 simulation length is 5 years and monthly average values are used for the analysis. First
451 consider the left plot. The TE tendency from parameterizations ($\partial\widehat{E}_{phys}^{(param)}$) show signif-
452 icant variability with an amplitude of approximately $2.5W/m^2$. As noted above this term
453 does not figure in the spurious TE budget. The net source/sink provides an equal and op-
454 posite term to balance it. That said, the variability is reflected onto the TE tendency due
455 to pressure work **error** $\partial\widehat{E}_{phys}^{(pwork)} \approx 0.32 \pm 0.08W/m^2$. On the scale used in the left-
456 hand plot the TE tendency of the adiabatic dynamical core $\partial\widehat{E}_{dyn}^{(adiab)}$ does not seem to be
457 affected by $\partial\widehat{E}_{phys}^{(param)}$ or $\partial\widehat{E}_{phys}^{(pwork)}$ in terms of variability, and remains stable at approxi-
458 mately $-0.6W/m^2 \pm 0.02W/m^2$. The TE fixer, in this model configuration, fixes $\partial\widehat{E}_{dyn}^{(adiab)}$
459 and $\partial\widehat{E}_{phys}^{(pwork)}$. Since the TE imbalance in the adiabatic dynamics remains approximately
460 constant and the TE tendency associated with pressure work **error** has variability, the TE
461 tendency from the $\partial\widehat{E}_{phys}^{(efix)}$ has variability; $\partial\widehat{E}_{phys}^{(efix)} \approx 0.30 \pm 0.08W/m^2$. As a consistency
462 check $-\partial\widehat{E}_{dyn}^{(adiab)} - \partial\widehat{E}_{phys}^{(pwork)}$ is plotted with asterisk's and they coincide (as expected)
463 with $\partial\widehat{E}_{phys}^{(efix)}$ fulfilling (23).

464 The right-hand plot in Figure 2 shows a breakdown of the dynamical core TE ten-
465 dencies. The majority of the TE errors are due to hyperviscosity on temperature and pres-
466 sure, $\partial\widehat{E}_{dyn}^{(hvis)} \approx -0.61 \pm 0.01W/m^2$. The diffusion of momentum is added back as fric-
467 tional heating and is therefore not part of $\partial\widehat{E}_{dyn}^{(hvis)}$. The frictional heating is a significant
468 term in the TE tendency budget $\partial\widehat{E}_{dyn}^{(fheat)} \approx 0.56 \pm 0.02W/m^2$ and exhibits some variabil-
469 ity but with a rather small amplitude. The remaining TE error in the floating Lagrangian
470 dynamics is inviscid dissipation and time-truncation errors $\partial\widehat{E}_{dyn}^{(res)} = \partial\widehat{E}_{dyn}^{(2D)} - \partial\widehat{E}_{dyn}^{(hvis)} \approx$
471 $0.007W/m^2$. The TE tendency from vertical remapping is approximately $\partial\widehat{E}_{dyn}^{(remap)} \approx$

473 $-0.01W/m^2$. To within $\sim 0.02W/m^2$ the dynamical core TE tendency terms can be com-
 474 puted from just one month average TE integrals. The TE tendencies computed in physics,
 475 excluding $\partial\widehat{E}_{phys}^{(param)}$, exhibit more variability and are only accurate to $\sim 0.1W/m^2$ after a
 476 one month average.

477 While it is advantageous to use *state-update* physics-dynamics coupling algorithm
 478 (`ftype=1`) in terms of having no spurious TE tendency from coupling, $\partial\widehat{E}^{(pdc)} = 0$,
 479 it does result in spurious gravity waves in the simulations [see, e.g., Figure 5 in *Gross*
 480 *et al.*, 2018]. Figure 3a shows a 1 year average of $|\frac{dps}{dt}|$, a measure of high frequency
 481 gravity wave noise. It clearly exhibits unphysical oscillations coinciding with element
 482 boundaries. Details of the spectral-element method, its coupling to physics and associ-
 483 ated noise issues are discussed in detail in *Herrington et al.* [2018]. The noise in the so-
 484 lutions is even visible in the 500hPa pressure velocity annual average (Figure 4a). This
 485 issue can be alleviated by using a shorter physics time-step so that the physics increments
 486 are smaller (not shown). Climate modelers have historically not pursued a shorter physics
 487 time-step in production configurations as climate parameterizations are computationally
 488 expensive and there is a large sensitivity to physics time-steps in the simulated climate
 489 [e.g. *Williamson and Olson*, 2003; *Wan et al.*, 2015].

490 3.2 ‘dribbling’ A/B: Non-TE conservative physics-dynamics coupling (`ftype=0, 2`)

491 Before discussing the impact of different PDC methods on the TE budget, we dis-
 492 cuss element boundary noise issues in CAM-SE which are related to PDC method.

493 3.2.1 *Spurious element boundary noise from physics-dynamics coupling*

494 When switching to *dribbling* physics-dynamics coupling algorithm (`ftype=0`) in
 495 which the tendencies from physics are added throughout the dynamics (in this case twice
 496 per physics time-step) then the noise issues described in previous section disappear (Figure
 497 3b and 4b). That said, there is a significant issue with this approach; the tracer mass bud-
 498 get may not be closed. How this comes about is illustrated in Figure 5 and explained in
 499 the next paragraph.

500 The orange curve on Figure 5a, b, d, and e is the initial state of, e.g., cloud liq-
 501 uid mixing ratio as a function of location, e.g., longitude. Cloud liquid is zero outside
 502 of clouds and hence provides a good example for the purpose of this illustration. The
 503 light blue arrows show the increments (in terms of length of arrow) computed by the
 504 parameterizations based on the initial state and scaled for the partial update with *dribbling*
 505 (`ftype=0`). With *state-update* (`ftype=1`) the increments from physics are added to the
 506 dynamical core state (dotted line on 5b) before the dynamical core advances the solution
 507 in time. The parameterizations are designed to not drive the mixing ratios negative so the
 508 state-update in dynamics will not generate negatives (or overshoots). Then the dynami-
 509 cal core advects the distribution (solid curve on Figure 5c). With *dribbling* (`ftype=0`) the
 510 physics increments are split into equal chunks (in this illustration two; blue errors on Fig-
 511 ure 5d). Half of the physics increments are added to the initial state (dotted line on Fig-
 512 ure 5e) and then dynamics advects the distribution half of the total dynamical core steps
 513 (dashed line on Figure 5e). Then the other half of the physics increments are applied (in
 514 the same location as they were computed by physics). Now after the previous/first advec-
 515 tion step the cloud liquid distribution has moved and the mixing ratio may be zero (or
 516 less than the increment prescribed by physics) where the physics forcing is applied (e.g.,
 517 left side of dashed curve). Hence the physics increment is driving the mixing ratios neg-
 518 ative in those locations. Thereafter the distribution is advected (solid curve on Figure 5f).
 519 In CAM the increments added in the dynamical core are limited so that they drive the
 520 mixing to zero (but not negative) if this problem occurs. This leads to a net source of
 521 mass compared to the mass change that the parameterizations prescribe (see Figure 6).
 522 Although the average source of mass is small each time-step it always has the same sign

(i.e. it is a bias) and therefore accumulates. *Zhang et al.* [2017] estimated that this spurious source of mass is equivalent to $\sim 10\text{cm}$ sea-level rise per decade in coupled climate simulation experiments.

The majority of the noise with *state-update* (`ftype=1`) physics-dynamics coupling method comes from momentum sources/sinks and heating/cooling. A way to alleviate noise problems and, at the same time, close the tracer mass budgets (in physics-dynamics coupling) is to use *state-update* (`ftype=1`) coupling for tracers and *dribbling* (`ftype=0`) coupling for momentum and temperature (referred to as *combination*, `ftype=2`). Figure 3c shows the noise diagnostic $|\frac{dp_s}{dt}|$ for *combination* (`ftype=2`) coupling. Figure 3c looks very similar to Figure 3b but there is some noise near element boundaries. That said, in terms of vertical pressure velocities *combination* (`ftype=2`) and *dribbling* (`ftype=0`) climates are similar in terms of the level of noise (Figure 4b and 4c). The element noise in CAM-SE with *combination* (`ftype=2`) seen in both $|\frac{dp_s}{dt}|$ and 500hPa pressure velocity can be ‘removed’ by using CAM-SE-CSLAM (Figure 3d) which uses a quasi equal-area physics grid and CSLAM [Conservative Semi-LAgrangian Multi-tracer; *Lauritzen et al.*, 2010] consistently coupled to the SE method [*Lauritzen et al.*, 2017]. The noise patterns in vertical velocity off the western coast of South America are present in all CAM-SE simulations (and hence not related to physics-dynamics coupling algorithm) are also ‘removed’ by using CAM-SE-CSLAM [*Herrington et al.*, 2018].

3.2.2 Spurious TE tendencies from physics-dynamics coupling

When using the same TE formula in the dynamical core and physics the spurious TE tendency from physics-dynamics coupling can be assessed. As described in item 5 (Section 2.2), PDC errors can be attributed to underlying pressure changes during the ‘dribbling’ of temperature and velocity component increments as well as PDC ‘clipping’ errors in the water variables (the process in which ‘clipping’ occurs is described in detail in the previous subsection). The TE error associated with ‘clipping’ PDC error occurs due to the mass-change prescribed by physics consistent with the fluxes in/out of the physics column does not equal the actual mass change applied to the dynamical core state due to ‘clipping’

For `ftype=2` PDC only the increment for temperature and momentum are *dribbled* and the PDC TE tendency is $\partial \widehat{E}^{(pdc)} = -0.484W/m^2$. When using `ftype=0` PDC also tracer increments are *dribbled*, which can lead to ‘clipping’ PDC TE errors, a similar TE tendency results $\partial \widehat{E}^{(pdc)} = -0.469W/m^2$. The difference between the TE PDC tenendency for `ftype=2` and `ftype=0` provides an estimate of the TE PDC ‘clipping’ error. The ‘clipping’ PDC TE tenendency is very small $0.015W/m^2$.

3.3 vert limiter: Limiters on vertical remapping of momentum

CAM-SE uses a floating Lagrangian vertical coordinate [*Starr*, 1945; *Lin*, 2004] which requires the remapping of the atmospheric state from floating levels back to reference levels to maintain computational stability and to provide state data consistent with the physics formulation. The mapping algorithm is based on the mass conservative PPM (Piecewise Parabolic Method) with options for shape-preserving limiters. In CAM-SE momentum components and internal energy are used as the variables mapped in the vertical [*Lauritzen et al.*, 2018] and, contrary to earlier versions of CAM-SE, there is no limiter on the remapping of wind components. If the shape-preserving limiter is used for momentum mapping then the TE dissipation increases by over an order of magnitude from $\sim 0.01W/m^2$ to $\sim 0.2W/m^2$ (Table 1).

569 3.4 *smooth topo*: Smoother topography

570 Topography for CAM is generated using a new version of the software/algorithm de-
 571 scribed in *Lauritzen et al.* [2015] that is available at <https://github.com/NCAR/Topo>.
 572 The updates to the software includes smoothing algorithms and the computation of sub-
 573 grid-scale orientation of topography.

574 The default topography in CAM-SE uses the same amount of topography smooth-
 575 ing as CAM-FV (distance weighted smoother applied to the raw topography on $\sim 3\text{km}$
 576 cubed-sphere grid with a smoothing radius of 180km referred to as C60). When the to-
 577 polography is smoother (in this case using C92 smoothing, i.e. smoothing radius of approx-
 578 imately 276km) the hyperviscosity operators are less active leading to reduced TE errors,
 579 i.e. $\partial\hat{E}^{(hv)}$ is reduced in half from approximately -0.6W/m^2 to -0.3W/m^2 . The vertical
 580 remapping TE error, however, remains approximately the same. Since the pressure work
 581 **error** is approximately 0.3W/m^2 it almost exactly compensates for the TE tendency from
 582 the dynamical core $\partial\hat{E}^{(adiab)}$. Hence if one would only diagnose the TE tendency from
 583 the energy fixer one could mistakenly conclude that the model universally conserves TE
 584 when, in fact, there are compensating TE errors in the system. These compensating errors
 585 can only be diagnosed through a careful breakdown of the total TE tendencies.

586 3.5 *default*: TE formula discrepancy errors

587 To assess the TE errors due to the discrepancy in the energy formula used by dy-
 588 namics and physics, a simulation using *state-updating* (*ftype*=1, no ‘dribbling’ errors) and
 589 thermodynamically/**inertially** active condensates in the dynamical core (*qsize_condensate_loading* =
 590 5) and consistent/accurate associated heat capacities $c_p^{(\ell)}$ (namelist *lcp_moist=true.*)
 591 has been performed. In this setup the continuous equations of motion in the dynami-
 592 cal core conserve an energy different from physics, and the energy fixer will restore the
 593 ‘physics’ version of energy. Despite the dynamical core now using a more comprehensive
 594 formula for energy, the TE dissipation terms in the dynamical core are roughly the same
 595 as in the energy consistent versions of the model. Using (26) we can assess the TE energy
 596 discrepancy errors which result in $\sim 0.59\text{W/m}^2$. *Taylor* [2011] found a similar result just
 597 from using the more comprehensive formula for heat capacity (based on dry air and water
 598 vapor) and not including thermodynamically/**inertially** active condensates. As noted before
 599 this formulation inconsistency is due to the evolutionary nature of CAM development and
 600 it is the intention to remove this inconsistency in future versions of the model.

601 The default version of CAM-SE uses this configuration but with *combination* (*ftype*=2)
 602 which has similar TE characteristics (see Table 1). That said, the physics-dynamics cou-
 603 pling error from *dribbling* momentum and temperature tendencies and the energy discrep-
 604 ency errors can not be separated in this configuration:

$$\partial\hat{E}^{(pdc)} + \partial\hat{E}^{(discr)} = 0.546\text{W/m}^2, \quad (27)$$

605 using (23). With *state-updating* (*ftype*=1) (i.e. $\partial\hat{E}^{(pdc)} = 0$) the energy discrepancy error
 606 was 0.594W/m^2 and in the energy consistent setup (i.e. $\partial\hat{E}^{(discr)} = 0$) but using *dribbling*
 607 (*ftype*=2) we got $\partial\hat{E}^{(pdc)} = 0.484\text{W/m}^2$. So if the physics-dynamics coupling errors
 608 and energy discrepancy errors in the different configurations would be additive, one would
 609 have expected $\partial\hat{E}^{(pdc)} + \partial\hat{E}^{(discr)}$ to be over 1W/m^2 which is clearly not the case (27).
 610 Again, it must be concluded that there are canceling errors in the system.

611 3.6 *QPC6*: Simplified surface

612 By running the model in aqua-planet configuration one can assess the effect of sim-
 613 plifying the surface boundary condition. In particular, without topography forcing the dy-
 614 namical core is not challenged with respect to stationary near-grid-scale forcing. The TE
 615 tendency with respect to pressure work **error** remains the same $\partial\hat{E}_{phys}^{(pwork)}$ as the AMIP-

616 type simulations, however, the adiabatic dynamical core TE tendency reduces to $\partial\widehat{E}_{dyn}^{(adiab)} =$
 617 $-0.14W/m^2$ (approximately a factor 4 reduction). Most of that reduction is due to viscosity
 618 $\partial\widehat{E}_{dyn}^{(visc)} = -0.13W/m^2$. The frictional heating is roughly the same as AMIP $\partial\widehat{E}_{dyn}^{(fheat)} =$
 619 $0.48W/m^2$ as is the vertical remapping $\partial\widehat{E}_{dyn}^{(remap)} = -0.01W/m^2$. To evaluate the dynam-
 620 ical cores diffusion of TE it is therefore important to asses the model in a configuration
 621 with topography as the wave dynamics generated by topography leads to more active dif-
 622 fusion operators.

623 3.7 FHS94: Simplified physics (no moisture)

624 Simplifying the setup even further by replacing the parameterizations with relax-
 625 ation towards a zonally symmetric temperature profile and simple boundary layer friction
 626 (Held-Suarez forcing) as well as excluding moisture, the TE errors in the dynamical core
 627 decreases even further to $\sim 0.002W/m^2$ since there is no small scale forcing. Small scales
 628 are only created by the nonlinear dynamics and the physics works to damp them. Hyper-
 629 viscosity is less active leading to significant reductions compared to aqua-planet and ‘real-
 630 world’ simulation results. The TE diffusion in vertical remapping reduces by an order of
 631 magnitude compared to the aqua-planet simulations ($\sim 0.0005W/m^2$). This further em-
 632 phasizes that TE diffusion assessment in a simplified setup is not necessarily telling for
 633 the dynamical cores performance with moist physics and topography that challenge the
 634 dynamical core in terms of strong grid-scale forcing.

635 3.8 FV: Changing dynamical core to Finite-Volume (FV)

636 As a comparison the TE error characteristics of the CAM-FV dynamical core are
 637 assessed. Although the TE diagnostics have not been implemented in the CAM-FV dy-
 638 namical core, the TE diagnostics in CAM physics are independent of dynamical core
 639 and can therefore be activated with CAM-FV. The CAM-FV dynamical core uses *state-*
 640 *update* physics-dynamics coupling (*ftype*=1) ($\partial\widehat{E}^{(pdc)} = 0$) and the same TE definition
 641 as CAM physics ($\partial\widehat{E}^{(discr)} = 0$). Hence (24) can be used to compute the TE errors of
 642 the CAM-FV dynamical core, $\partial\widehat{E}_{dyn}^{(adiab)} \approx -1W/m^2$. As we do not have the break-down
 643 of $\partial\widehat{E}_{dyn}^{(adiab)}$ it can not be determined how much of the TE errors are due to the vertical
 644 remapping. Furthermore, CAM-FV contains intrinsic dissipation operators (limiters in the
 645 flux operators) making it difficult to assess TE sources/sinks due to dissipation. Note that
 646 the pressure work **error** even with a change of dynamical core remains approximately the
 647 same as the CAM-SE configurations.

648 3.9 CSLAM: Quasi equal-area physics grid

649 This configuration was discussed in the context of element noise in section 3.2.1.
 650 By averaging the dynamics state of an equal-partitioning (in central angle cubed-sphere
 651 coordinates) of the elements, the element-boundary noise found in CAM-SE can be re-
 652 moved. Lauritzen *et al.* [2018] argue that this way of computing the state for the physics
 653 is more consistent with physics in terms of providing a cell-averaged state instead of ir-
 654 regularly spaced point (quadrature) values. In order to achieve a closed mass-budget, this
 655 configuration uses CSLAM for tracer transport rather than SE transport. That said, the
 656 physics columns no longer coincide with the quadrature grid and there are TE errors asso-
 657 ciated with mapping state and tendencies between the two grids.

658 In this configuration the energy diagnostics computed in the dynamical core are
 659 computed on the quadrature grid and the energy diagnostics computed in physics are on
 660 the physics grid. If the TE consistent configuration is used (*ftype*=1, *qsize_condensate_loading*=1,
 661 *lcp_moist*=.false.) then the physics-dynamical coupling errors, $\widehat{E}^{(pdc)}$ computed with
 662 (21), are entirely due to mapping state from quadrature grid to physics grid and map-

663 ping tendencies back the quadrature grid from the physics grid. The results is $\widehat{E}^{(pdc)} =$
 664 $-0.07W/m^2$ which is a rather small error compared to other terms in the TE budget.

665 Due to similar noise problems with CAM-SE-CSLAM when using ftype=1 that
 666 were observed in CAM-SE (Figure 3 and 4), the default version of CAM-SE-CSLAM uses
 667 ftype=2. Again physics-dynamics coupling errors and TE discrepancy errors can not be
 668 separated; $\partial\widehat{E}^{(pdc)} + \partial\widehat{E}^{(discr)} = 0.557W/m^2$.

671 4 Conclusions

672 A detailed total energy (TE) error analysis of the Community Atmosphere Model
 673 (CAM) using version 6 physics (included in the CESM2.1 release) running at approxi-
 674 mately 1° horizontal resolution has been presented. In the global climate model there can
 675 be many spurious contributions to the TE budget. These errors can be divided into four
 676 categories: physical parameterizations, adiabatic dynamical core, the coupling between
 677 physics and dynamics, and TE definition discrepancies between dynamics and physics.
 678 The latter is not by design but through the evolutionary nature of model development. By
 679 capturing the atmospheric state at various locations in the model algorithm, a detailed
 680 budget of TE errors can be constructed. The net spurious TE energy errors are com-
 681 pensated with a global energy fixer (providing a global uniform temperature increment) every
 682 physics time-step.

683 In CAM physics the parameterizations have, by design, a closed energy budget (change
 684 in TE is balanced by fluxes in/out the top and bottom of physics columns) if it is assumed
 685 that pressure is not modified. However, the pressure changes due to fluxes of mass (e.g.,
 686 water vapor) in/out of the column which changes energy (referred to as pressure work
 687 **error**). The pressure work **error** with the full moist physics configuration is very stable
 688 across different configurations at $\sim 0.3W/m^2$. The TE errors in the spectral element (SE)
 689 dynamical core varies across configurations. Aspects that influence TE is the presence
 690 of topography, the amount of topography smoothing and moist physics. By smoothing
 691 topography more the TE error is cut in half from $\sim -0.6W/m^2$ to $\sim -0.3W/m^2$; and re-
 692 duces by a factor of **six** ($\sim -0.1W/m^2$) if no topography is present at all (aqua-planet
 693 configuration). Moist physics forcing also contributes significantly to the TE budget. For
 694 example, in the dry Held-Suarez setup TE dissipation of the SE dynamical core reduces
 695 to $-0.03W/m^2$. Topography and moist physics force the dynamical core at the grid scale
 696 and hence the viscosity operators are more active. Consistent with this statement is that
 697 the changes in TE discussed so far are almost entirely due to the viscosity operator TE
 698 dissipation. For CAM-SE the spurious TE dissipation in the adiabatic dynamical core is
 699 $\sim -0.6W/m^2$ in ‘real-world’ configurations. For comparison, CAM-FV’s spurious TE
 700 change due to the adiabatic dynamical core is $\sim -1W/m^2$.

701 By further breaking down the TE dissipation in the SE dynamical core it is ob-
 702 served the vertical remapping accounts for only $\sim -0.01W/m^2$. That said, if the shape-
 703 preserving limiters in the vertical remapping are invoked the TE dissipation increases 20-
 704 fold to $\sim -0.2W/m^2$. In CAM-SE the kinetic energy dissipation is added as heating in
 705 the thermodynamic equation (also referred to as frictional heating). The frictional heat-
 706 ing remains very stable across configurations that include moisture ($\sim 0.5W/m^2$) and re-
 707 duces drastically for dry atmosphere setups (factor 4 reduction to ($\sim 0.12W/m^2$)). Hence
 708 this term is an important term in the TE budget. The TE budget for the dynamical core
 709 is dominated by TE change due to hyperviscosity; TE errors due to time-truncation and
 710 frictionless equations of motion are negligible. Errors associated with physics-dynamics
 711 coupling (if applicable) are approximately $0.5W/m^2$. Due to the evolutionary nature of
 712 model development the SE dynamical core’s continuous equation of motion conserve a
 713 more comprehensive TE compared to the physical parameterizations. This TE discrep-
 714 ency leads to an approximately $0.5W/m^2$ total energy source. Running physics on a dif-
 715 ferent grid than the dynamical introduces TE mapping errors such as in CAM-SE-CSLAM

(Conservative Semi-Lagrangian Multi-tracer transport scheme). These errors are, however, rather small $-0.07W/m^2$.

A purpose of this paper is to better understand the energy characteristics of CAM and to encourage modeling groups to perform similar analysis to better understand the total energy flow in the atmospheric component of Earth system models. As has been demonstrated in this paper there can easily be compensating errors in the system which can not be identified without a detailed TE analysis.

Acknowledgments

The National Center for Atmospheric Research is sponsored by the National Science Foundation. Computing resources ([doi:10.5065/D6RX99HX](https://doi.org/10.5065/D6RX99HX)) were provided by the Climate Simulation Laboratory at NCAR's Computational and Information Systems Laboratory, sponsored by the National Science Foundation and other agencies. The data used to perform the energy analysis can be found at <https://github.com/PeterHjortLauritzen/2018-JAMES-energy>.

References

- Boville, B. (2000), chap. Toward a complete model of the climate system in Numerical Modeling of the Global Atmosphere in the Climate System, pp. 419–442, Springer Netherlands.
- Computational and Information Systems Laboratory (2017), Cheyenne: HPE/SGI ICE XA System (Climate Simulation Laboratory), Boulder, CO: National Center for Atmospheric Research, doi:10.5065/D6RX99HX.
- Eldred, C., and D. Randall (2017), Total energy and potential enstrophy conserving schemes for the shallow water equations using hamiltonian methods – part 1: Derivation and properties, *Geosci. Model Dev.*, 10(2), 791–810, doi:10.5194/gmd-10-791-2017.
- Gross, M., H. Wan, P. J. Rasch, P. M. Caldwell, D. L. Williamson, D. Klocke, C. Jablonowski, D. R. Thatcher, N. Wood, M. Cullen, B. Beare, M. Willett, F. Lemarié, E. Blayo, S. Malardel, P. Termonia, A. Gassmann, P. H. Lauritzen, H. Johansen, C. M. Zarzycki, K. Sakaguchi, and R. Leung (2018), Physics-dynamics coupling in weather, climate and earth system models: Challenges and recent progress, *Mon. Wea. Rev.*, 146, 3505–3544, doi:10.1175/MWR-D-17-0345.1.
- Held, I. M., and M. J. Suarez (1994), A proposal for the intercomparison of the dynamical cores of atmospheric general circulation models, *Bull. Amer. Meteor. Soc.*, 75, 1825–1830.
- Herrington, A. R., P. H. Lauritzen, M. A. Taylor, S. Goldhaber, B. E. Eaton, K. A. Reed, and P. A. Ullrich (2018), Physics-dynamics coupling with element-based high-order Galerkin methods: quasi equal-area physics grid, *Mon. Wea. Rev.*
- Jablonowski, C., and D. L. Williamson (2011), chap. The Pros and Cons of Diffusion, Filters and Fixers in Atmospheric General Circulation Models, pp. 381–493, Springer Berlin Heidelberg, Berlin, Heidelberg, doi:10.1007/978-3-642-11640-7_13.
- Kasahara, A. (1974), Various vertical coordinate systems used for numerical weather prediction, *Mon. Wea. Rev.*, 102(7), 509–522.
- Lauritzen, P. H., R. D. Nair, and P. A. Ullrich (2010), A conservative semi-Lagrangian multi-tracer transport scheme (CSLAM) on the cubed-sphere grid, *J. Comput. Phys.*, 229, 1401–1424, doi:10.1016/j.jcp.2009.10.036.
- Lauritzen, P. H., J. T. Bacmeister, T. Dubos, S. Lebonnois, and M. A. Taylor (2014), Held-Suarez simulations with the Community Atmosphere Model Spectral Element (CAM-SE) dynamical core: A global axial angular momentum analysis using Eulerian and floating Lagrangian vertical coordinates, *J. Adv. Model. Earth Syst.*, 6, doi: 10.1002/2013MS000268.

- 766 Lauritzen, P. H., J. T. Bacmeister, P. F. Callaghan, and M. A. Taylor (2015), NCAR_Topo
 767 (v1.0): NCAR global model topography generation software for unstructured grids,
 768 *Geosci. Model Dev.*, 8(12), 3975–3986, doi:10.5194/gmd-8-3975-2015.
- 769 Lauritzen, P. H., M. A. Taylor, J. Overfelt, P. A. Ullrich, R. D. Nair, S. Goldhaber, and
 770 R. Kelly (2017), CAM-SE-CSLAM: Consistent coupling of a conservative semi-
 771 lagrangian finite-volume method with spectral element dynamics, *Mon. Wea. Rev.*,
 772 145(3), 833–855, doi:10.1175/MWR-D-16-0258.1.
- 773 Lauritzen, P. H., R. Nair, A. Herrington, P. Callaghan, S. Goldhaber, J. Dennis, J. T.
 774 Bacmeister, B. Eaton, C. Zarzycki, M. A. Taylor, A. Gettelman, R. Neale, B. Dobbins,
 775 K. Reed, and T. Dubos (2018), NCAR release of CAM-SE in CESM2.0: A reformu-
 776 lation of the spectral-element dynamical core in dry-mass vertical coordinates with
 777 comprehensive treatment of condensates and energy, *J. Adv. Model. Earth Syst.*, doi:
 778 10.1029/2017MS001257.
- 779 Lin, S.-J. (2004), A 'vertically Lagrangian' finite-volume dynamical core for global mod-
 780 els, *Mon. Wea. Rev.*, 132, 2293–2307.
- 781 McRae, A. T. T., and C. J. Cotter (2013), Energy- and enstrophy-conserving schemes for
 782 the shallow-water equations, based on mimetic finite elements, *Quart. J. Roy. Meteor.
 783 Soc.*, 140(684), 2223–2234, doi:10.1002/qj.2291.
- 784 Medeiros, B., D. L. Williamson, and J. G. Olson (2016), Reference aquaplanet climate in
 785 the community atmosphere model, version 5, *J. Adv. Model. Earth Syst.*, 8(1), 406–424,
 786 doi:10.1002/2015MS000593.
- 787 Neale, R. B., and B. J. Hoskins (2000), A standard test for AGCMs including their phys-
 788 ical parametrizations: I: the proposal, *Atmos. Sci. Lett.*, 1(2), 101–107, doi:10.1006/asle.
 789 2000.0022.
- 790 Neale, R. B., C.-C. Chen, A. Gettelman, P. H. Lauritzen, S. Park, D. L. Williamson, A. J.
 791 Conley, R. Garcia, D. Kinnison, J.-F. Lamarque, D. Marsh, M. Mills, A. K. Smith,
 792 S. Tilmes, F. Vitt, P. Cameron-Smith, W. D. Collins, M. J. Iacono, R. C. Easter, S. J.
 793 Ghan, X. Liu, P. J. Rasch, and M. A. Taylor (2012), Description of the NCAR Commu-
 794 nity Atmosphere Model (CAM 5.0), *NCAR Technical Note NCAR/TN-486+STR*, National
 795 Center of Atmospheric Research.
- 796 Skamarock, W. C., J. B. Klemp, M. G. Duda, L. Fowler, S.-H. Park, and T. D. Ringler
 797 (2012), A multi-scale nonhydrostatic atmospheric model using centroidal Voronoi tes-
 798 selations and C-grid staggering, *Mon. Wea. Rev.*, 240, 3090–3105, doi:doi:10.1175/
 799 MWR-D-11-00215.1.
- 800 Starr, V. P. (1945), A quasi-Lagrangian system of hydrodynamical equations., *J. Atmos.
 801 Sci.*, 2, 227–237.
- 802 Taylor, M. A. (2011), Conservation of mass and energy for the moist atmospheric prim-
 803 itive equations on unstructured grids, in: P.H. Lauritzen, R.D. Nair, C. Jablonowski,
 804 M. Taylor (Eds.), Numerical techniques for global atmospheric models, *Lecture Notes
 805 in Computational Science and Engineering*, Springer, 2010, *in press.*, 80, 357–380, doi:
 806 10.1007/978-3-642-11640-7_12.
- 807 Thuburn, J. (2008), Some conservation issues for the dynamical cores of NWP and cli-
 808 mate models, *J. Comput. Phys.*, 227, 3715–3730.
- 809 Trenberth, K. E., and J. T. Fasullo (2018), Applications of an updated atmospheric ener-
 810 getics formulation, *J. Climate*, 31(16), 6263–6279, doi:10.1175/JCLI-D-17-0838.1.
- 811 Wan, H., P. J. Rasch, M. A. Taylor, and C. Jablonowski (2015), Short-term time step con-
 812 vergence in a climate model, *J. Adv. Model. Earth Syst.*, 7(1), 215–225, doi:10.1002/
 813 2014MS000368.
- 814 Williamson, D. L. (2002), Time-split versus process-split coupling of parameterizations
 815 and dynamical core, *Mon. Wea. Rev.*, 130, 2024–2041.
- 816 Williamson, D. L., and J. G. Olson (2003), Dependence of aqua-planet simulations on
 817 time step, *Q. J. R. Meteorol. Soc.*, 129(591), 2049–2064.
- 818 Williamson, D. L., J. G. Olson, C. Hannay, T. Toniazzo, M. Taylor, and V. Yudin (2015),
 819 Energy considerations in the community atmosphere model (cam), *J. Adv. Model. Earth*

- 820 *Syst.*, 7(3), 1178–1188, doi:10.1002/2015MS000448.
821 Zhang, K., P. J. Rasch, M. A. Taylor, H. Wan, L.-Y. R. Leung, P.-L. Ma, J.-C. Golaz,
822 J. Wolfe, W. Lin, B. Singh, S. Burrows, J.-H. Yoon, H. Wang, Y. Qian, Q. Tang,
823 P. Caldwell, and S. Xie (2017), Impact of numerical choices on water conservation in
824 the e3sm atmosphere model version 1 (eam v1), *Geoscientific Model Development Dis-*
825 *cussions*, 2017, 1–26, doi:10.5194/gmd-2017-293.

```

do nt=1,ntotal

PARAMETERIZATIONS:
Last dynamics state received from dynamics
output 'pBF'
efix Energy fixer
output 'pBP'
phys param Physics updates the state and state saved for energy fixer
output 'pAP'
pwork Pressure work (dry mass correction)
output 'pAM'
Physics tendency (forcing) passed to dynamics

DYNAMICAL CORE
output 'dED'
do ns=1,nsplit
output 'dAF'

phys
START PHYSICS-DYNAMICS COUPLING
Update dynamics state with (1/nsplit) of physics tendency (ftype=2)
if (ns=1) Update dynamics state with entire physics tendency (ftype=1)
DONE PHYSICS-DYNAMICS COUPLING

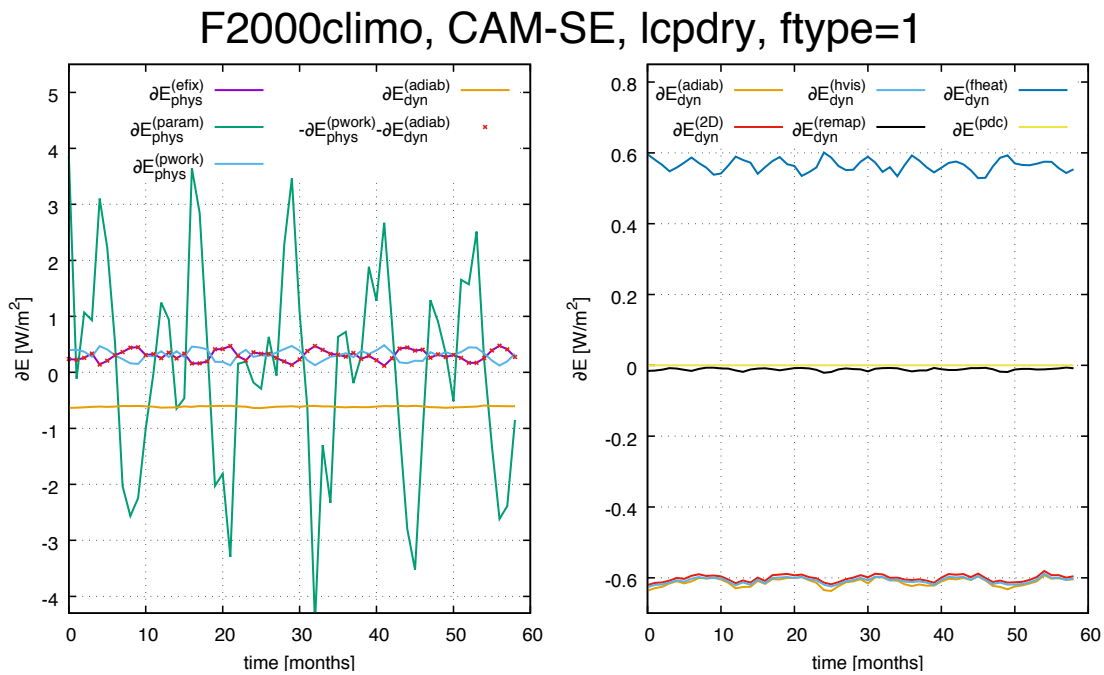
output 'dB'D'

adiab
2D
hvis
do nr=1,rsplit
Advance the adiabatic frictionless equations of motion
in floating Lagrangian layer
do ns=1,hypervis_subcycle
output 'dBH'
Apply hyperviscosity operators
output 'dCH'
fheat Add frictional heating to temperature
output 'dAH'
end do (ns=1,hypervis_subcycle)
end do (nr=1,rsplit)
output 'dAD'
remap
Vertical remapping from floating Lagrangian levels to Eulerian levels
output 'dAR'
end do (ns=1,nsplit)
Dynamics state saved for next model time step and passed to physics
output 'dB'F'

end do (nt=1,ntotal)

```

283 **Figure 1.** Pseudo-code for CAM-SE showing the order in which relevant physics updates are performed as
284 well as dynamical core steps and associated loops. In green font locations where the state is captured and out-
285 put is shown together with its 3 character identifier. The outer most loop (1, *ntotal*) advances the entire model
286 Δt_{phys} seconds (in this case 1800s). The dynamical core loops are as follows: the outer loop is the vertical
287 remapping loop (1, *nsplit*) with associated time-step $\Delta t_{phys}/nsplit$. For stability the temporal advance-
288 ment of the equations of motion in the Lagrangian layer needs to be sub-cycled *rsplit* times. Within the
289 *rsplit*-loop the hyperviscosity time-stepping is sub-cycled *hypervis_subcycle* times (again for stability).
For more details on the time-stepping in CAM-SE see Lauritzen *et al.* [2018].



432 **Figure 2.** Monthly averaged TE tendencies as a function of time for various aspects of the TE consistent
 433 configuration of CAM-SE run in AMIP-type configuration with perpetual year 2000 SSTs. Left Figure shows
 434 $\partial \hat{E}$ TE tendencies in physics and, for comparison, TE tendency for the adiabatic dynamical core. The right
 435 plot shows the break-down of $\partial \hat{E}$ for the dynamical core. These plots show that the energy tendency from the
 436 dynamical core is quite constant (to within $\sim 0.02 W/m^2$ or less) so only one month simulations is adequate to
 437 assess energy diagnostics for the dynamical core. For more details see Section 3.1.

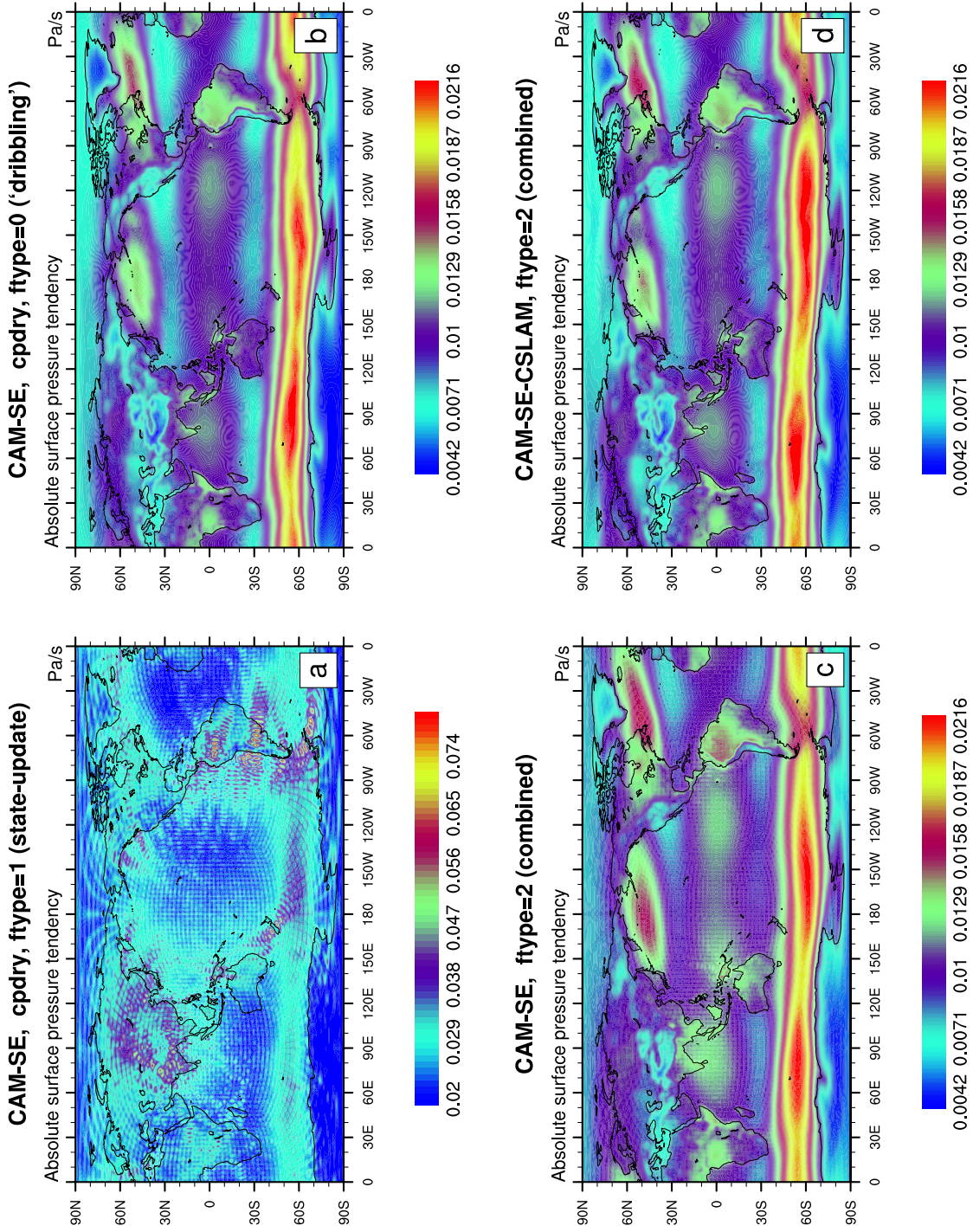


Figure 3. One year average of the absolute surface pressure tendency for (a) the TE consistent configuration, (b) ‘dribbling’ physics-dynamics coupling, (c) ftype=2 physics-dynamics coupling and (d) CSLAM version of CAM-SE, respectively. (a) has a closed physics-dynamics coupling budget but spurious noise, (b) has no spurious noise but the mass-budget in physics-dynamics coupling is not closed (see Figure 6), (c) has a closed mass budget in physics-dynamics coupling but some spurious noise at element boundaries which is eliminated when using CAM-SE-CSLAM (d). Note, the smallest value in panel (a) is the largest in panels (b), (c) and (d).

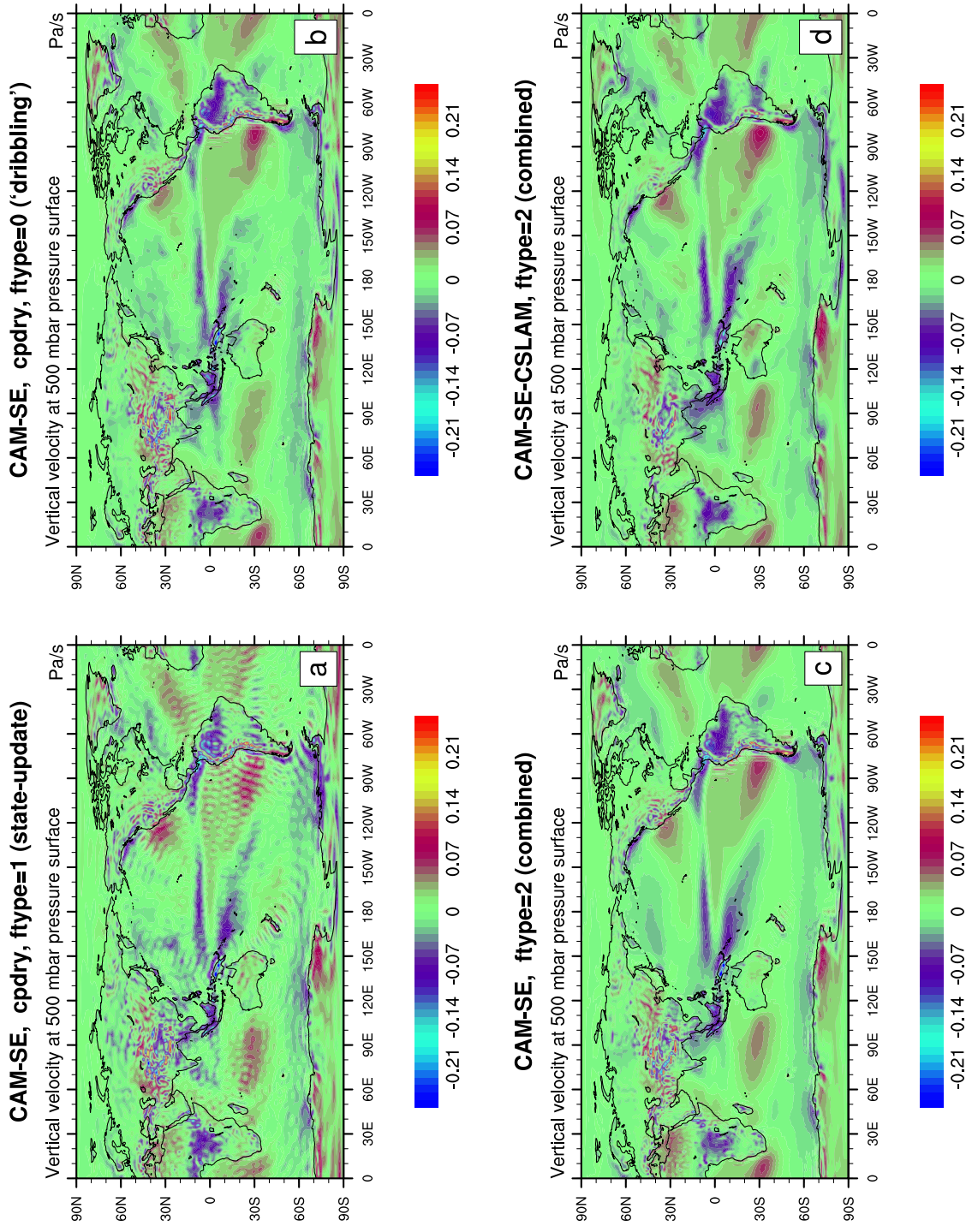
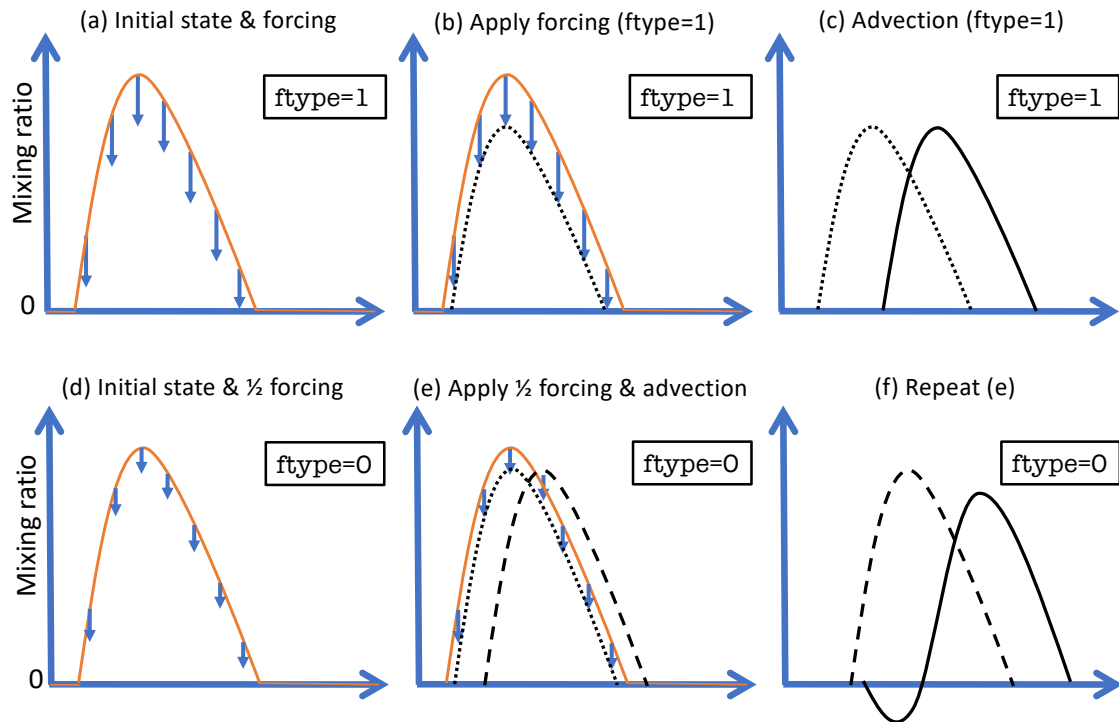


Figure 4. Same as Figure 3 but for 500hPa vertical pressure velocity. Note the ringing patterns off the West coast of South America and around the Himalayas in CAM-SE (a-c) that are eliminated with CAM-SE-CSLAM (d) that makes use of a quasi equal-area physics grid.



669 **Figure 5.** A schematic of state-update ($\text{ftype}=1$; row 1) and ‘dribbling’ ($\text{ftype}=0$; row 2) physics-
670 dynamics coupling algorithms. See Section 3.2 for details.

F2000climo, CAM-SE, cpdry, ftype=0 ('dribbling')

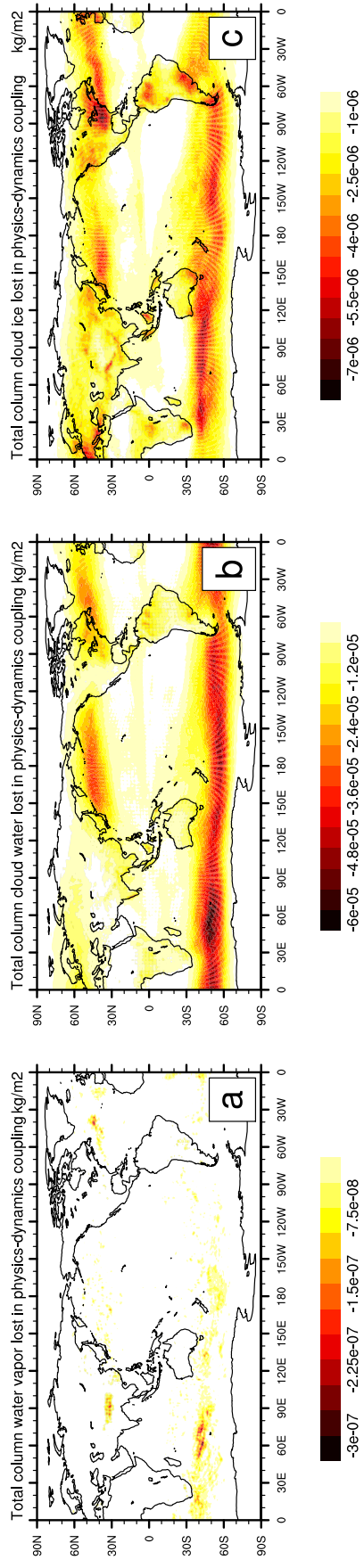


Figure 6. One year average of mass $[kg/m^2]$ 'clipped' in physics-dynamics coupling (so that state is not driven negative) when using `ftype=0` ('dribbling') physics-dynamics coupling for (a) water vapor, (b) cloud liquid and (c) cloud ice, respectively. Interestingly the element boundaries systematically show in the plots which is likely related to the anisotropy of the quadrature grid [Herrington *et al.*, 2018].